Phase partitioning initiates Rab protein membrane domain formation and promote vesicle tethering

Ana Joaquina Jimenez[1]*, Franck Perez[1]*

[1] Institut Curie, PSL Research University, CNRS, UMR 144, Dynamics of Intracellular Organization, F-75005, Paris, France;
*Corresponding authors: ana-joaquina.jimenez@curie.fr , franck.perez@curie.fr

Abstract
Cellular processes are regulated by the formation of specific membrane domains with different lipid and protein compositions. Small GTPases play a role in symmetry breaking and compartmentalization, with early endosomes presenting Rab5-enriched domains that regulate vesicle tethering and fusion. Rabaptin5, which binds activated Rab5 and forms dimers, is essential for endosome fusion and promotes Rab5 recruitment to membranes. Liquid-liquid phase separation (LLPS) is a mechanism for the biogenesis and maintenance of membrane-less organelles and intracellular organization. We show that several partners of Rab proteins, such as Rabaptin5, have phase-separation properties. In particular, Rabaptin5 form condensates close to membranes, while promoting the enrichment of several Rabs involved in early steps of endocytosis. We propose that phase separation of Rab partners ensures efficient recruitment of their respective Rabs and domain formation and maintenance.

Introduction
A variety of cellular processes are regulated by the formation of specific membrane domains with different lipid and protein composition. There is abundant evidence of the existence of domains enriched in specific small GTPases and involved in symmetry breaking and compartmentalization like Cdc42, Rop11 and Rab5. Particularly, early endosomes present Rab5 enriched domains where Rab5 regulates vesicle tethering and fusion [1–3]. A role of CapZ in endosome tethering through the regulation of actin nucleation has also been described [4].

Small GTPases cycle from soluble to membrane bound depending on their GDP or GTP state. The GDP soluble form high affinity complexes with guanine dissociation inhibitors (GDI) [5–7]. This cycling is regulated by guanine nucleotide exchange factors (GEFs), which ensures the exchange from GDP to GTP, and by GTPase activating proteins (GAPs), which accelerate the hydrolysis of the GTP into GDP [5,8]. Several examples have also described Rab GEFs interaction with Rab effectors possibly triggering feed-forward loops of their own recruitment, like for example Rab5 GEF Rabex5 with Rab5 effector Rabaptin5 [9]. Those GEF/Effector interactions have also been suggested to be a general mechanism for domain formation and symmetry breaking [10]. Nevertheless, to our knowledge, no experimental data has been described supporting any model leading Rab domain formation.

Among Rabs, the Rabex5/Rabaptin complex has been best studied [9,11,12]. Rabaptin5 is essential for endosome fusion (Stenmark et al., 1995; Horiuchi et al., 1997), and several

interaction domains of Rabaptin5 have been mapped among them a domain binding activated Rab5, another domain binding Rab5 and a domain binding Rabex5 [13]. In addition, Rabaptin5 is also able to form dimers (Lauer et al. 2019). All these interactions contribute to a feed forward loop of Rab5 recruitment to membranes by bringing closer Rab5 to its GEF and to already activated and membrane bound Rab5, likely promoting biased binding of Rab5-GTP to membranes and promoting domain formation [3,14]. The interaction of Rabaptin5 with Rabex5 has been shown to produce structural changes on Rabex5 structure and potentiate its activity [9,11,12,15–17]. Besides a possible first step of this domain formation may pass through Rabex5 recruitment to Early Endosomes (EE) via two distinct Ubiquitin binding domains [18].

In the past few years, liquid-liquid phase separation (LLPS) has emerged in the field of cellular biology as a powerful mechanism for the biogenesis and maintenance of membrane-less organelles like nucleoli, pBodies or stress granules (Banani 2017 from Ede1 paper), creating that way intracellular organization and membrane less compartmentalization [19]. Phase separation is also a powerful mechanism to maintain protein concentration stable and to recruit molecules from their cytoplasmic pool (Lyon 2021 from Ede1). A study in yeast suggests that Ede1 (Eps15 in mammalian) condensates promotes the neoformation and maturation of endocytic sites [20]. *In vitro* studies also suggest the implication of Eps15 and Fcho1/2 and their LLPS properties in endocytosis initiation [21]. Another study show that the Rab6 effector ELKS has phase separation properties that promote the recruitment of other actors of the polarized membrane associated platforms (PMAPs) near cell edges [22]. Finally, LLPS of Nephrin, apposed to membranes, was shown to increase dwell time of N-Wasp and Arp2/3 potentiating Actin filament nucleation [23]. Similarly, the activation of Ras has been shown to be potentiated by partner condensates formed on membranes [24]. Here we show that several partners of Rab proteins have phase-separation properties. Those proteins present similar characteristics with long coil-coiled domains and unstructured domains, similar to Ede1. Taking the example of Rabaptin5, we show that Rabaptin5 condensates form close to membranes (plasma membrane and endosomal membranes) and that they promote the enrichment of several Rab involved in early steps of endocytosis: Rab4 and Rab5 enrichment. Condensates from partners related to different Rabs present partial or no co-condensation. We propose that phase separation of Rab effectors ensure efficient recruitment of their respective Rabs and domain formation and maintenance.

Results and discussion

A continuum of evolving membranes, which transform into each other, constitutes intracellular membranes involved in traffic. Rab proteins are involved in domain biogenesis and constitute good markers of the identity state of those membranes (Fig. 1A). Rab5, among the most studied Rabs, is present in domains on Early Endosomes and is involved in the regulation of membrane tethering and fusion [2,3]. Feed-forward loops involving Rab5 GEF Rabex5 and Rab5 effector Rabaptin5 are believed to establish Rab5 domains (Fig. 1B). The predicted structure of Rabaptin5 (Alphafold) anticipates the presence of long alpha helices and unstructured domains (Fig. 1C). Disorder analysis by different algorithms predicts a high disorder score, with a highly disorder larger domain in the middle of the protein (Fig. 1D), but unlike Ede1, no prion-like domain was detected using PLAAC software. We investigated the

response of Rabaptin5 distribution to increase in extracellular osmolarity induced by sucrose, NaCl, or sorbitol, and we observed that Rabaptin5, initially uniformly distributed in the cytoplasm, formed condensates upon an increase in extracellular medium osmolarity (Fig. 1E), even with small increases in osmolarity.

The size of Rabaptin5 condensates increased with the concentration of extracellular medium (Fig. 2A-F) as measured by the standard deviation of the fluorescence within the cell (Fig. 2B,D,F). Osmotic stress triggered by NaCl addition required lower concentrations than sucrose or sorbitol osmotic stresses (Fig. 2A-F) and started at very low concentrations of NaCl. Condensate growth is also time-dependent as low concentrations of sucrose that did not trigger LLPS, did eventually after longer incubations (Fig. 3A-B). mApple-Rabaptin5 condensates were observed in cells with very different levels of expression, although in low expressing cells they required different acquisition settings to be detectable, suggesting that many LLPS condensates are not detected with commonly used acquisition settings. The size of condensates was higher in cells expressing high levels of Rabaptin5 (Fig. 3C). Many condensates grew from pre-existing Rabaptin5 faint puncta suggesting that Rabaptin5 condensates were already present at steady state (Fig. 3D). Condensates presented commonly accepted LLPS characteristics: reversibility (Fig. 4A,B) and the capacity to undergo fusion (Fig. 4C) and fission (Fig. 4D). Interestingly some fusion events occurred faster than others (Fig. 4C). Rabaptin5 is highly conserved among the whole animal kingdom but its amino acid sequence is less conserved in insects with only ~25% identity and up to ~45% similarity (identity included) (Fig. 5A, Fig. 6A). Despite this divergence, structure prediction reveals striking similarities (Fig. 5B, Fig. 6B-C) and when expressed in mammalian cells using a humanized sequence of Drosophila ortholog, the resulting protein has also phase separation properties upon osmotic stress (Fig. 5C) and condensates also grow from pre-existing faint Drosophila-Rabaptin5 positive patches (Fig. 5D). We tested also truncated versions of Rabaptin5 described before [13], and interestingly only dual truncation of the protein for both N-terminal and C-terminal could abolish its phase separation capacities (data not shown).
We check that LLPS was not a general reaction of all proteins to osmotic stress. Soluble EGFP did not react to sucrose addition (Fig. 7A) nor did mCherry-CHMP4B (Fig. 7C), which is capable of oligomerization [25]. Although Clathrin did not react massively to osmotic stress, we could observe an increase in intensity of Clathrin puncta (Fig. 7B). Interestingly, Rab5 was enriched in Rabaptin5 positive condensates (Fig. 7D), as well as Rab4 (data not shown) consistent with described interactions between Rabaptin5 and Rab4 [13]. We could also observe that Rab5 effector Rabenosyn5, which is known to be involved in endosomal fusion [26], has also LLPS properties (Fig. 7E). In order to have better resolution on the possible interaction of Rabaptin5 domains and Rab5 positive endosomes, we induced enlarged endosomes by overexpressing Rab5Q79L using enlarged endosomes, we could also observe that Rabaptin5 condensates occur asymmetrically in endosomes and most of the time accompanied by similar Rab5 asymmetry in cells with isosmotic conditions (Fig. 8A-C) or hyperosmotic stress (Fig. 8D-F). Besides, induction of Rabaptin5 condensates by sucrose addition induced novel Rabaptin5-Rab5 domains on enlarged endosomes as evident by comparing scan lines of endosome contours before and after sucrose addition (Fig. 8C,F), especially in panel e where there is no Rabaptin5 condensate previous to sucrose addition but many of them after), suggesting that Rabaptin5 condensates promote Rab5 domain formation on discrete portions of endosomal membranes. We could also observe that Rabaptin5 condensates could tether two endosomes together (Fig. 8 G,H). This observation and the fact that Rabenosyn5 (Fig.7 E) is also able to

make condensates and promotes fusion made us hypothesize that LLPS may have a tethering function in endosomes. This may explain previous observations of oligomeric complexes involved in tethering of endosomes [2]. Although we could not observe any CapZ recruitment do Rabaptin5 condensates, we do not exclude that condensates could be a mechanism to enrich CapZ and modulate actin polymerization on endosomes.

Furthermore, we could observe that besides on endosomes, Rabaptin5 condensates can be found close to edges (Fig. 9A), suggesting that Rabaptin5 condensates happen docked to membranes similarly of what was observed in other systems [23,24]. Interestingly, Rabaptin5 condensates only partially co-localized with EEA1-FYVE domain and Rab5 (Fig. 9B,C) and while EEA1-FYVE and Rab5 were preferentially localized inside the cells, Rabaptin5 condensates were found preferentially at the edges (Fig. 9B,C), suggesting that those condensates form upstream of Rab5 mature endosomes. Besides, Rabaptin5 condensates did not co-localize with late endosome markers like Rab7 (data not shown).
Next, to check whether Rabaptin5 condensates could appear in any Rabaptin5 containing membrane, we used an indirect system to not add additional interactions to Rabaptin5, and we used the FRB-FKBP system to artificially recruit small amounts of Rabex5 to the Golgi apparatus using Rab6 or a truncated version of Giantin as hooks (Fig. 10 A,B) and we could observe that Rabex5 recruitment induced the recruitment of small amount of Rabaptin5 at the Golgi apparatus (Fig. 10B,D middle panel). Upon increase in extracellular medium osmolarity we could observe an enrichment of Rabaptin5 at the Golgi apparatus but the condensates at the periphery of the cell were always stronger (Fig. 10 B,D, lower panels) suggesting that membranes at cell edges are more suitable to host Rabaptin5 condensates than membranes downstream in the retrograde traffic pathway, suggesting again that Condensates of Rabaptin5 have a role in early stages of endocytosis.

We then checked the possibility that all Rab domains may be generated through partner LLPS. Among the partners we tested, many of them presented LLPS properties. Interestingly all the ones empowered with LLPS properties presented predicted long coil-coiled domains and unstructured portions (Fig. 11 A-D), namely two partners of Rab6, ELKS and BICD1 (Fig. 11A,B), and two partners of Rab4, RUFY1 and GRASP1 (Fig. 11C,D). In a lesser extent, RILP, also presented LLPS properties (data not shown). Interestingly, condensates of partners of early markers of endocytosis like GRASP1 co-condensated with Rabaptin5 (Fig. 11G), while partners of Rabs involved in later stages of retrograde trafficking did not (Fig. 11F) or only partially (Fig. 11E) co-localised. Most interestingly, Rabaptin5 condensates were found to partially co-localise with ELKS at focal adhesions suggesting once again its very early position in retrograde membranes.

All together, we bring strong evidence that Rab proteins are in partnership with proteins with LLPS capacities. With the example of Rabaptin5, we show that LLPS are capable of inducing Rab domains and vesicle tethering. Besides, sometimes side-by side, condensates of different partners may co-condensate or stay unmixed suggesting a role in mixing and de-mixing their Rab partners. We propose a model LLPS rules the establishment of Rab membrane domains and tethering of vesicles.

Figure Legends:

Figure 1. The Rab5 partner Rabaptin presents disordered domains and liquid-liquid-phase separation properties.
A. Continuum of Rab domains during endocytosis. B. Current model for Rab5 feed-forward loop recruitment. C. Structure prediction of Rabaptin 5 by Aphafold. D. Disorder prediction using the indicated algorithms. E. HeLa cells were transfected with EGFP-Rabaptin5 and treated with different kinds of extra cellular medium osmolarity increase as indicated.

Figure 2. Levels of Rabaptin5 responses to increase in osmolarity depend on extracellular osmolarity.
HeLa cells were transfected with EGFP-Rabaptin5 and treated with different kinds of extra cellular medium osmolarity increase as indicated. Responses to increasing concentrations of A-B. Sucrose, C-D. NaCl and E-F. Sorbitol. Responses start at very low osmolarity increase.

Figure 3. Levels of Rabaptin5 responses with time exposure at low concentrations of sucrose.
HeLa cells were transfected with EGFP-Rabaptin5 and treated with different kinds of extra cellular medium osmolarity increase as indicated. A-B. Time-dependent response of Rabaptin5 to low Sucrose. C. Rabaptin5-Concentration dependent response to Sucrose, but consistent in all levels of expression tested, which require different levels of visualization. D. Condensates grow from pre-existing structures.

Figure 4. Rabaptin5 Condensates are reversible and can undergo Fusion and Fission
HeLa cells were transfected with EGFP-Rabaptin5 and treated with different kinds of extra cellular medium osmolarity increase as indicated. A. Reversibility. B. Fusion events. C. Fission events.

Figure 5. Rabaptin5 LLPS property is conserved in Drosophila despite high amino-acid divergence.
A. Comparison with Rabaptin5 protein in other species. B. Comparision of the predicted structure (Alphafold) of Homo sapiens and Drosophila melanogaster Rabaptin5. C. HeLa cells were transfected with mApple-Drosophila Rabaptin5 and treated as indicated. D. Condensates grow from pre-existing structures.

Figure 6. Amino acid sequence of Rabaptin5 is less conserved in Drosophila but its structure is.
A. Alignment of Homo sapiens and Drosophila melanogaster Rabaptin5 protein. B. Alphafold predicted structure. C. Alignment following similar predicted structural domains.

Figure 7. LLPS is not a "by-default" property of proteins involved in endocytosis.
HeLa cells were transfected with indicated plasmids and treated with 187µM Sucrose.

Figure 8. Rabaptin5 LLPS takes place on endosome membranes and triggers Rab5 domain formation.
HeLa cells were co-transfected with EGFP-Rabaptin5 and mCherry-Rab5 Q79L. A,B,C. Before Sucrose addition. D,E,F,G. After Sucrose addition. G. show and example of tethering event by Rabaptin5 condensates. H. Corresponding Scheme of G.

Figure 9. Rabaptin5 condensates emerge mostly close to the plasma membrane and not on pre-existing PI(3)P domains.
HeLa cells were transfected as indicated and treated with 187µM of Sucrose.

Figure 10. Rabaptin5 recruitment to Golgi apparatus membranes is not sufficient to launch strong emergence observed at the plasma membrane.
HeLa cells were transfected as indicated and treated with Rapamycin for 10min then with 187µM of Sucrose. A-C. Scheme of the experiment performed in B-D.

Figure 11. Other Rab partners present similar predicted caracteristics and similar LLPS but each partnet has its own condensate signature.
HeLa cells were transfected as indicated and treated with 187µM of Sucrose.

Figure 12. Proposed model.

Materials and Methods

Cell Culture and transfection

HeLa cells were grown in Dulbecco's modified Eagle (DMEM) medium (Gibco BRL) supplemented with 10% fetal bovine serum (Biowest) and 1mM sodium pyruvate, 100 µg/ml penicillin/streptomycin (Invitrogen). Cells were seeded onto 6-well plates, 25mm glass coverslips and transfected in suspension. For expression of the constructs used in this study, HeLa cells were transfected using calcium phosphate precipitates as previously described [27]. For increase in medium osmolarity cells were treated with indicated concentrations with Sucrose, Sorbitol or NaCl (Merck)

Construction of DNA plasmids
Construction of plasmids are by the moment available upon request.

Time lapse fluorescence microscopy
Prior to transfection, HeLa cells were seeded on glass coverslips with a diameter of 25 mm and transfected in suspension. After 20 hours of transfection with the appropriate plasmids, the coverslips were moved to an L-shaped tubing Chamlide from Live Cell Instrument, which was filled with pre-warmed Leibovitz's medium that is independent of carbonate (manufactured by Invitrogen). At indicated time point, hyperosmotic media was added to the chamber using the tubing. Time-lapse acquisitions were captured at 37 °C within a thermostat-controlled chamber, utilizing an Eclipse 80i microscope from Nikon that is equipped with a spinning disk confocal head from Perkin and a iXon (Andor) camera from Gataca Systems. Images were acquired using MetaMorph software from Molecular Device, with a 100× objective.

Image Analysis
Custom ImageJ macros were used to mount and analyse the images. Integrated intensity or standard deviation was measured at every time point in a region of interest (ROI), in the

resulting sum of an acquired z-stack. Curves were performed using R-Studio or Prism (Graphpad) softwares. Figures were done using Affinity Designer Software.

Acknowledgements:
We thank Marino Zerial, Martin Spiess and Valentina Millarte for sharing Rabaptin5 plasmids. We thank Peter van der Sluijs for Grasp1 and Rufy1 plasmids; Marci Scidmore for BICD1 plasmid from Addgene # 49487; Terence Dermody, Bernardo Mainou for Addgen plasmid # 110498; Silvia Corvera for Addgene plasmid # 37538 ; Ron Vale and Marino Zerial for Addgene plasmid # 31733 and Rab5 Q79L plasmid. Guillaume Montagnac for Clathrin plasmid. Simon de Becco and Mathieu Coppey for EEA1-Fyve domain plasmid; Anna Akhmanova for the ELKS plasmid.
We also thank Ahmed ElMarjou and Berengère Ouine for their help with Rabaptin5 purification and Bruno Goud for discussion; Séverine Divoux for ongoing Electron-microscopy experiments.

Bibliography:

1. Franke C, Repnik U, Segeletz S, Brouilly N, Kalaidzidis Y, Verbavatz J, Zerial M: **Correlative single-molecule localization microscopy and electron tomography reveals endosome nanoscale domains**. *Traffic Cph Den* 2019, **20**:601–617.

2. McBride HM, Rybin V, Murphy C, Giner A, Teasdale R, Zerial M: **Oligomeric complexes link Rab5 effectors with NSF and drive membrane fusion via interactions between EEA1 and syntaxin 13**. *Cell* 1999, **98**:377–386.

3. Sönnichsen B, De Renzis S, Nielsen E, Rietdorf J, Zerial M: **Distinct Membrane Domains on Endosomes in the Recycling Pathway Visualized by Multicolor Imaging of Rab4, Rab5, and Rab11**. *J Cell Biol* 2000, **149**:901–914.

4. Wang D, Ye Z, Wei W, Yu J, Huang L, Zhang H, Yue J: **Capping protein regulates endosomal trafficking by controlling F-actin density around endocytic vesicles and recruiting RAB5 effectors**. *eLife* 2021, **10**:e65910.

5. Cherfils J, Zeghouf M: **Regulation of small GTPases by GEFs, GAPs, and GDIs**. *Physiol Rev* 2013, **93**:269–309.

6. Ghomashchi F, Zhang X, Liu L, Gelb MH: **Binding of prenylated and polybasic peptides to membranes: affinities and intervesicle exchange**. *Biochemistry* 1995, **34**:11910–11918.

7. Sasaki T, Kikuchi A, Araki S, Hata Y, Isomura M, Kuroda S, Takai Y: **Purification and characterization from bovine brain cytosol of a protein that inhibits the dissociation of GDP from and the subsequent binding of GTP to smg p25A, a ras p21-like GTP-binding protein**. *J Biol Chem* 1990, **265**:2333–2337.

8. Bos JL, Rehmann H, Wittinghofer A: **GEFs and GAPs: critical elements in the control of small G proteins**. *Cell* 2007, **129**:865–877.

9. Horiuchi H, Lippé R, McBride HM, Rubino M, Woodman P, Stenmark H, Rybin V, Wilm M, Ashman K, Mann M, et al.: **A novel Rab5 GDP/GTP exchange factor complexed to Rabaptin-5 links nucleotide exchange to effector recruitment and function**. *Cell* 1997, **90**:1149–1159.

10. Goryachev AB, Leda M: **Autoactivation of small GTPases by the GEF-effector positive feedback modules**. *F1000Research* 2019, **8**:F1000 Faculty Rev-1676.

11. Delprato A, Lambright DG: **Structural basis for Rab GTPase activation by VPS9 domain exchange factors**. *Nat Struct Mol Biol* 2007, **14**:406–412.

12. Lauer J, Segeletz S, Cezanne A, Guaitoli G, Raimondi F, Gentzel M, Alva V, Habeck M, Kalaidzidis Y, Ueffing M, et al.: **Auto-regulation of Rab5 GEF activity in Rabex5 by allosteric structural changes, catalytic core dynamics and ubiquitin binding**. *eLife* 2019, **8**.

13. Kälin S, Hirschmann DT, Buser DP, Spiess M: **Rabaptin5 is recruited to endosomes by Rab4 and Rabex5 to regulate endosome maturation**. *J Cell Sci* 2015, **128**:4126–4137.

14. Cezanne A, Lauer J, Solomatina A, Sbalzarini IF, Zerial M: **A non-linear system patterns Rab5 GTPase on the membrane**. *eLife* 2020, **9**.

15. Delprato A, Merithew E, Lambright DG: **Structure, exchange determinants, and family-wide rab specificity of the tandem helical bundle and Vps9 domains of Rabex-5**. *Cell* 2004, **118**:607–617.

16. Lippé R, Horiuchi H, Runge A, Zerial M: **Expression, purification, and characterization of Rab5 effector complex, rabaptin-5/rabex-5**. *Methods Enzymol* 2001, **329**:132–145.

17. Zhang Z, Zhang T, Wang S, Gong Z, Tang C, Chen J, Ding J: **Molecular mechanism for Rabex-5 GEF activation by Rabaptin-5**. *eLife* 2014, **3**.

18. Penengo L, Mapelli M, Murachelli AG, Confalonieri S, Magri L, Musacchio A, Di Fiore PP, Polo S, Schneider TR: **Crystal structure of the ubiquitin binding domains of rabex-5 reveals two modes of interaction with ubiquitin**. *Cell* 2006, **124**:1183–1195.

19. Lyon AS, Peeples WB, Rosen MK: **A framework for understanding the functions of biomolecular condensates across scales**. *Nat Rev Mol Cell Biol* 2021, **22**:215–235.

20. Kozak M, Kaksonen M: **Condensation of Ede1 promotes the initiation of endocytosis**. *eLife* 2022, **11**:e72865.

21. Day KJ, Kago G, Wang L, Richter JB, Hayden CC, Lafer EM, Stachowiak JC: **Liquid-like protein interactions catalyse assembly of endocytic vesicles**. *Nat Cell Biol* 2021, **23**:366–376.

22. Sala K, Corbetta A, Minici C, Tonoli D, Murray DH, Cammarota E, Ribolla L, Ramella M, Fesce R, Mazza D, et al.: **The ERC1 scaffold protein implicated in cell motility drives the assembly of a liquid phase**. *Sci Rep* 2019, **9**:13530.

23. Case LB, Zhang X, Ditlev JA, Rosen MK: **Stoichiometry controls activity of phase separated clusters of actin signaling proteins**. *Science* 2019, **363**:1093–1097.

24. Huang WYC, Alvarez S, Kondo Y, Lee YK, Chung JK, Lam HYM, Biswas KH, Kuriyan J, Groves JT: **A molecular assembly phase transition and kinetic proofreading modulate Ras activation by SOS**. *Science* 2019, **363**:1098–1103.

25. Teis D, Saksena S, Emr SD: **Ordered assembly of the ESCRT-III complex on endosomes is required to sequester cargo during MVB formation**. *Dev Cell* 2008, **15**:578–589.

26. Nielsen E, Christoforidis S, Uttenweiler-Joseph S, Miaczynska M, Dewitte F, Wilm M, Hoflack B, Zerial M: **Rabenosyn-5, a Novel Rab5 Effector, Is Complexed with Hvps45 and Recruited to Endosomes through a Fyve Finger Domain**. *J Cell Biol* 2000, **151**:601–612.

27. Jordan M, Schallhorn A, Wurm FM: **Transfecting mammalian cells: optimization of critical parameters affecting calcium-phosphate precipitate formation**. *Nucleic Acids Res* 1996, **24**:596–601.

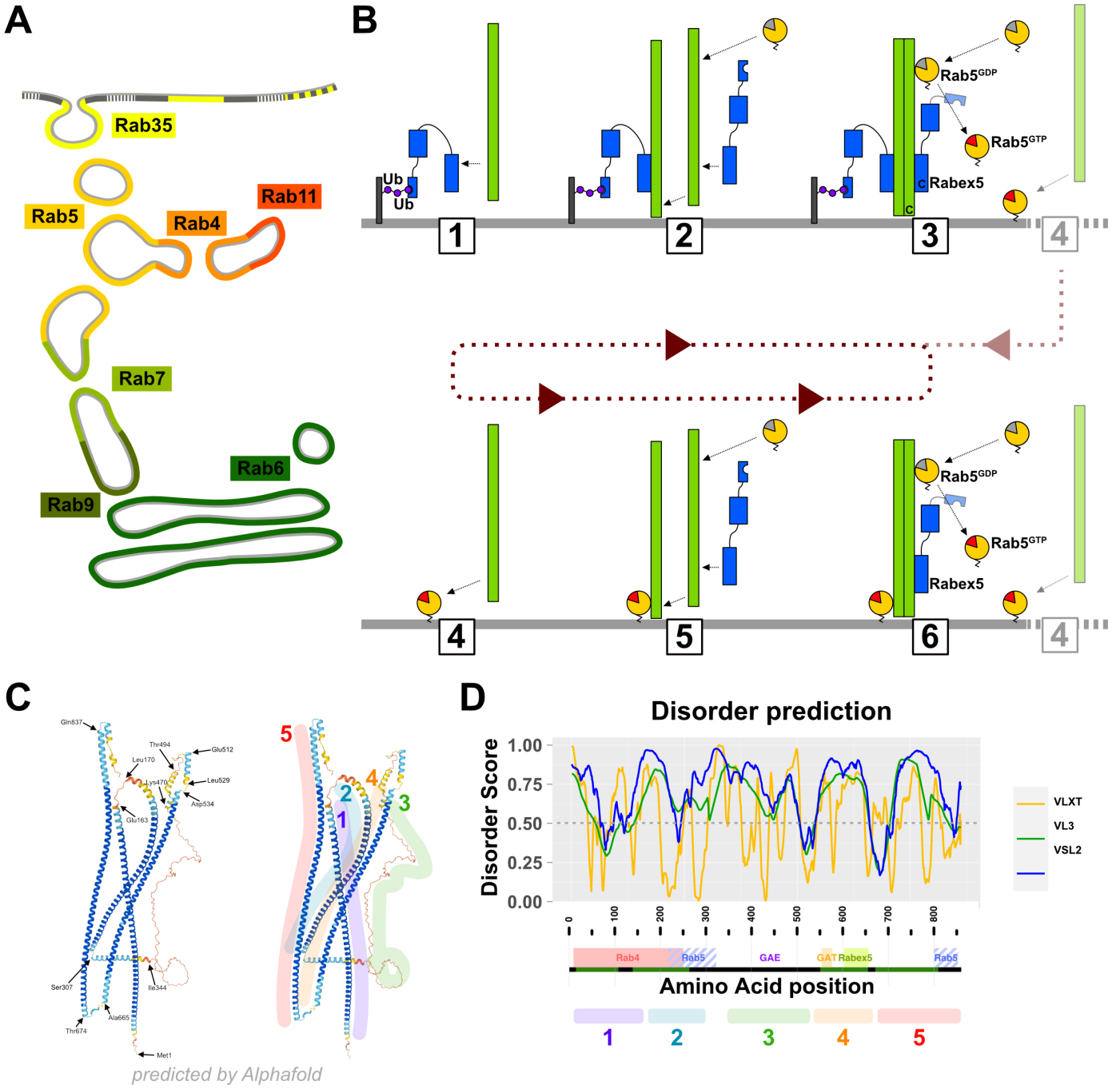

E Rabaptin phase separates upon osmotic shock

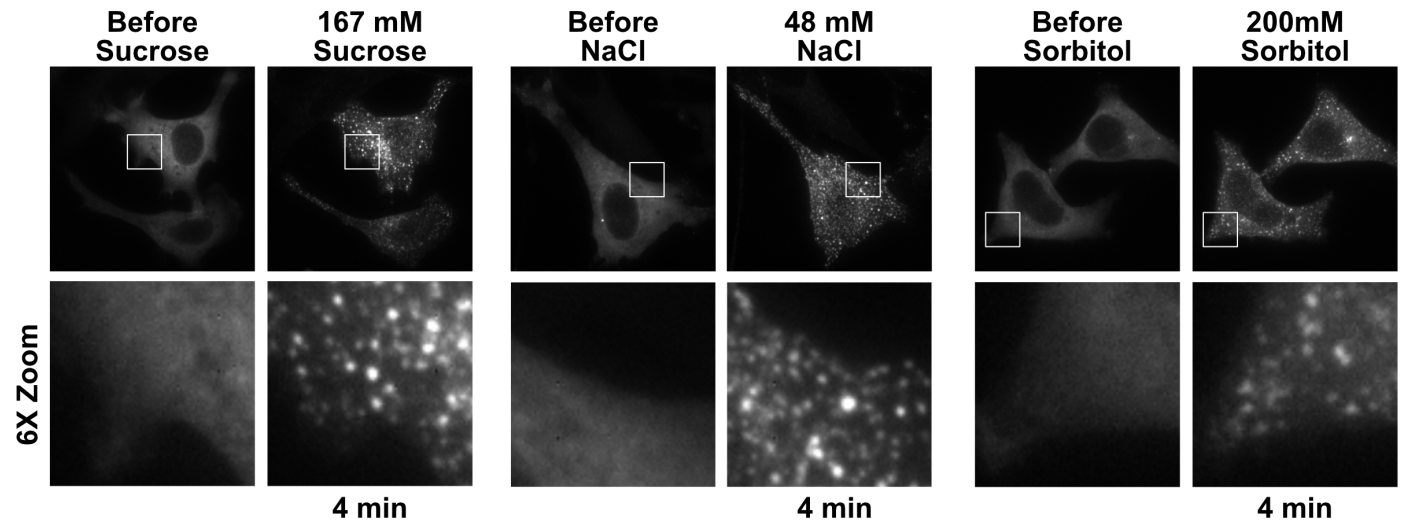

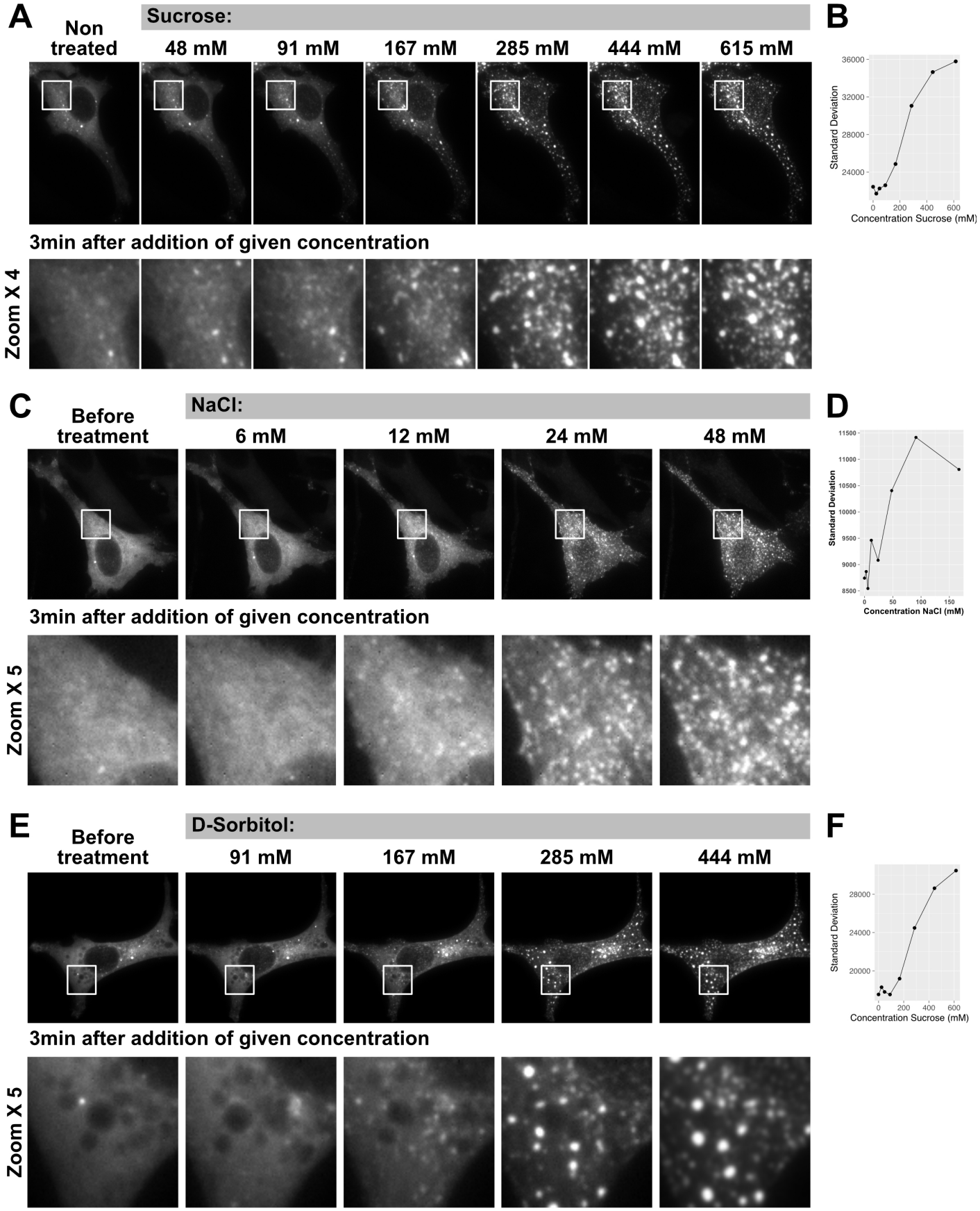
A
Sucrose:
Non treated
48 mM
91 mM
167 mM
285 mM
444 mM
615 mM
3min after addition of given concentration
Zoom X 4
B
Standard Deviation
Concentration Sucrose (mM)
C
NaCl:
Before treatment
6 mM
12 mM
24 mM
48 mM
3min after addition of given concentration
Zoom X 5
D
Standard Deviation
Concentration NaCl (mM)
E
D-Sorbitol:
Before treatment
91 mM
167 mM
285 mM
444 mM
3min after addition of given concentration
Zoom X 5
F
Standard Deviation
Concentration Sucrose (mM)

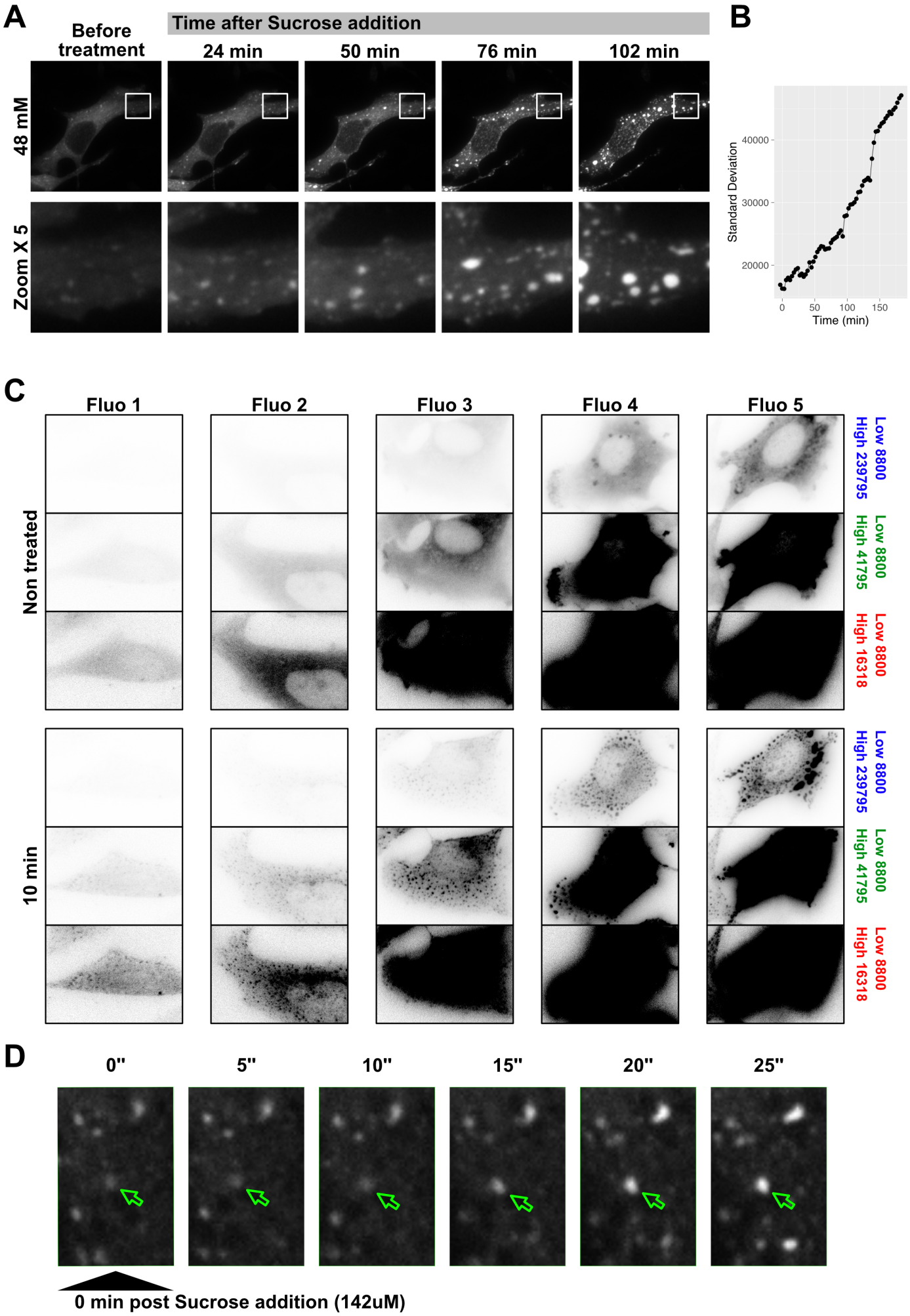
A
Before treatment
Time after Sucrose addition
24 min
50 min
76 min
102 min
48 mM
Zoom X 5
B
Standard Deviation
40000
30000
20000
0
50
100
150
Time (min)
C
Fluo 1
Fluo 2
Fluo 3
Fluo 4
Fluo 5
Non treated
10 min
Low 8800
High 239795
Low 8800
High 41795
Low 8800
High 16318
D
0"
5"
10"
15"
20"
25"
0 min post Sucrose addition (142uM)

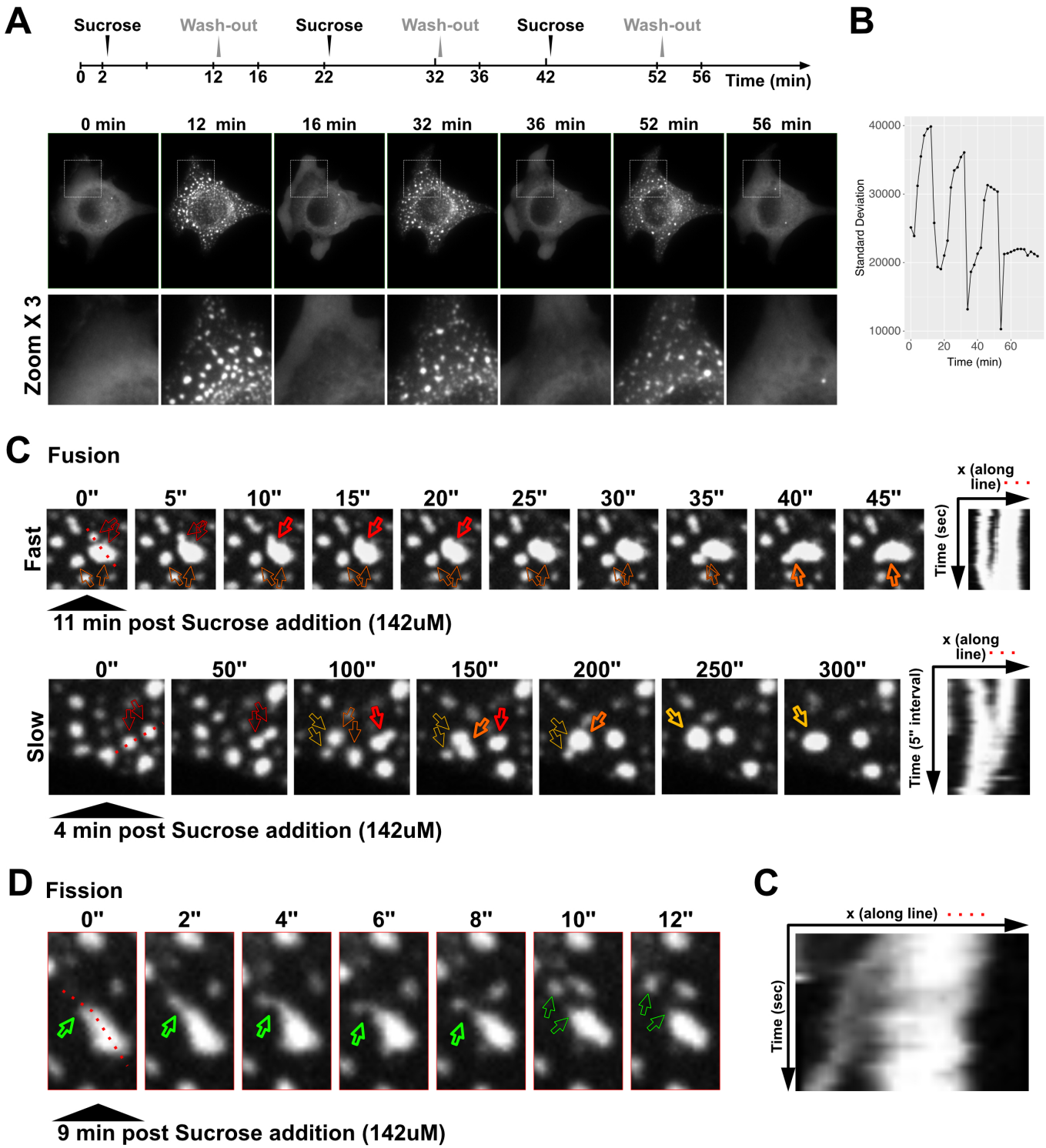
A
Sucrose
Wash-out
Sucrose
Wash-out
Sucrose
Wash-out
0 2 12 16 22 32 36 42 52 56 Time (min)
0 min
12 min
16 min
32 min
36 min
52 min
56 min
Zoom X 3
B
Standard Deviation
40000
30000
20000
10000
0 20 40 60
Time (min)
C Fusion
0" 5" 10" 15" 20" 25" 30" 35" 40" 45"
Fast
x (along line)
Time (sec)
11 min post Sucrose addition (142uM)
0" 50" 100" 150" 200" 250" 300"
Slow
x (along line)
Time (5" interval)
4 min post Sucrose addition (142uM)
D Fission
0" 2" 4" 6" 8" 10" 12"
9 min post Sucrose addition (142uM)
C
x (along line)
Time (sec)

A

	Length	% identity with H. sapiens Isoform1	% Similarity with H. sapiens Isoform1	Gaps compared to H. sapiens Isoform1
Homo sapiens Isoform1	862			
Rattus norvegicus	862	95,94%	98,03%	0%
Mus musculus isoform1	862	96,29%	98,26%	0%
Bos taurus	862	97,22%	98,96%	0%
Gallus gallus	860	88,05%	93,62%	0,23%
Xenopus tropicalis	853	77,73%	88,40%	1,04%
Danio renio isoform1	850	71,07%	83,47%	2,13%
Drosophila melanogaster	634	24,92%	45,43%	14,04%

B

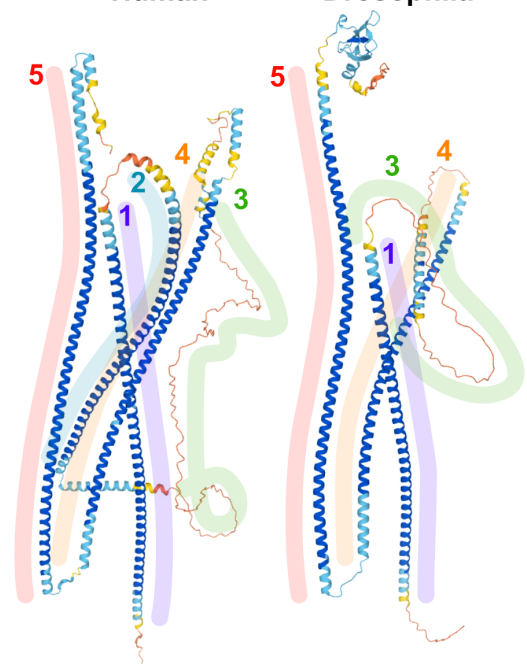

C

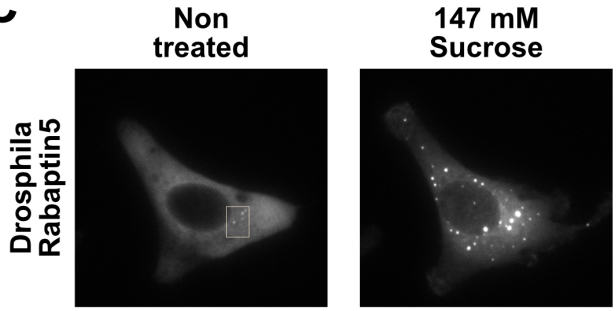

D

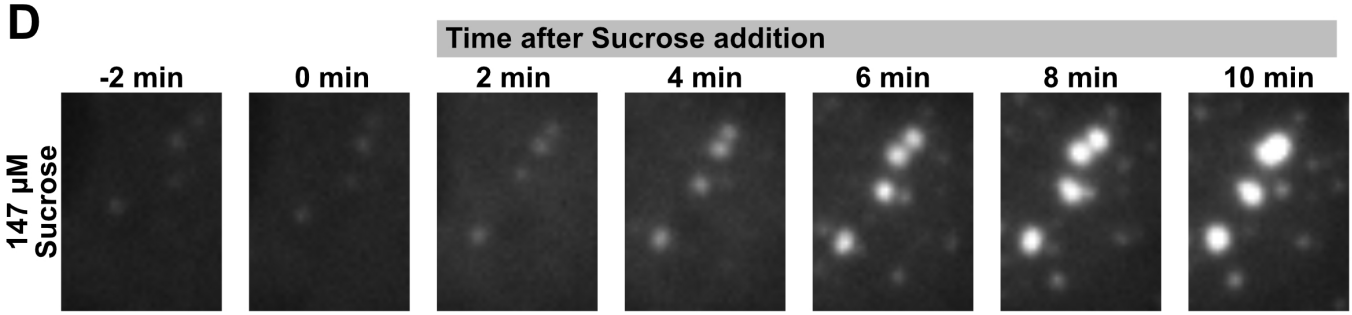

A

```
H. sapiens
D. melano.

1   MAQPG-----------PASQPDVSLQQRVAELEKINAEFLRAQQQLEQEFNQKRAKFKELYLAKEEDLKRQNAVLQAAQDDLGHLRTQLW  79
1   MEENETRSEAREPTDLPNGEDDATSQHKLSHLQ-------NEMRKMQNEFNTQRAKMRELYIQKEAE------VSQSQQE-----RRQL-  71

80  EAQAEMENIKAIATVSENTKQEAIDEVKRQWREEVASLQAVMKETVRDYEHQFHLRLEQERTQWAQYRESAEREIADLRRRLSEGQEEEN  169
71  --QAELDELKTHLMVADLKSQNELQLRDLKAQEEISSLQQLVQDTIEETAH-YKGEVERLRLELGKYQQIQQQTMAQQPQAESSGGIAPQ  158

170 LENEMKKAQEDAEKLRSVVMPMEKEIAALKDKLTEAEDKIKELEASKVKELNHYLEAEKSCRTDLEMYVAVLNTQKSVLQEDAEKLRKEL  259
159 VLNQVKKTLGSVRKLGT-------------DSLNSSFQQDEDTRASS------------------------KGNGKQYAPEEAEM----M  207

260 HEVCHLLEQERQQHNQLKHTWQKANDQFLESQRLLMRDMQRMEIVLTSEQLRQVEELKKKDQEDDEQQRLNKRKDHKKADVEEEIKIPVV  349
208 HSIVEQLQEE-------------------------------------------MKALKVKLREQDEQ-----------------------  231

350 CALTQEESSAQLSNEEEHLDSTRGSVHSLDAGLLLPSGDPFSKSDNDMFKDGLRRAQSTDSLGTSGSLQSKALGYNYKAKSAGNLDESDF  439
231 ---------------------------------------------------------------------------LQAKSAS--DES--  241

440 GPLVGADSVSENFDTASLGSLQMPSGFMLTKDQERAIKAMTPEQEETASLLSSVTQGMESAYVSPSGYRLVSETEWNLLQKEVHNAGNKL  529
241 -----ALHKSTSMDVA-------------------------------------------ESA---------------------------  255

530 GRRCDMCSNYEKQLQGIQIQEAETRDQVKKLQLMLRQANDQLEKTMKDKQELEDFIKQSSEDSSHQISALVLRAQASEILLEELQQGLSQ  619
255 ---CESCSLAEKKTEELGAHINKQQKQVDLLQKQLVESRETLVKEAALRKDLEDQWQEKREAHKSEVQSLRDQAKTNEQRLLDMQQKFLE  342

620 AKRDVQEQMAVLMQSREQVSEELVRLQKDNDSLQGKHSLHVSLQQAEDFI-LPDTTEALRELVLKYREDIINVRTAADHVEEKLKA---E  705
343 TKDEVIKQIQRVSDDRERVNKQLETLQADNDFLSGRY-LATSEEIDNQYINLPNTVVELQELILRQQSELIQARVSSEYERQKCTSTEDE  431

706 ILFLKEQIQAEQCLKENLEETLQLEIENCKEEIASISSLKAELERIKVEKGQLESTLREKSQQLESLQEIKISLEEQLKKETAAKATVEQ  795
432 IQILRAQLEESNNERRAYKRKMQLDIKSLQDR---VTEHLVTVQAYETTKTQLERKEAELNKQLSECRVEIIELQEANEKYAKTNA----  514

796 LMFEEKNKAQRLQTELDVSEQVQRDFVKLSQTLQVQLERIRQADSLER--------------------IRAI-------------LNDT-  851
514 ---DYKTKIKTLQEELSTMETVQKDFVKLSQTLQMSLEELRHADTEVRWQDDDDVNNCPTCNAYFTVMVRKIHCRHCGHIYCDKCLTKTV  601

851 ---------KLTDI--------------------------NQLPET  862
602 PSGPRKRVARVCDICHTLLTPNTAPYFSQGQPPQQQQGQQQQQQSN  647
```

B

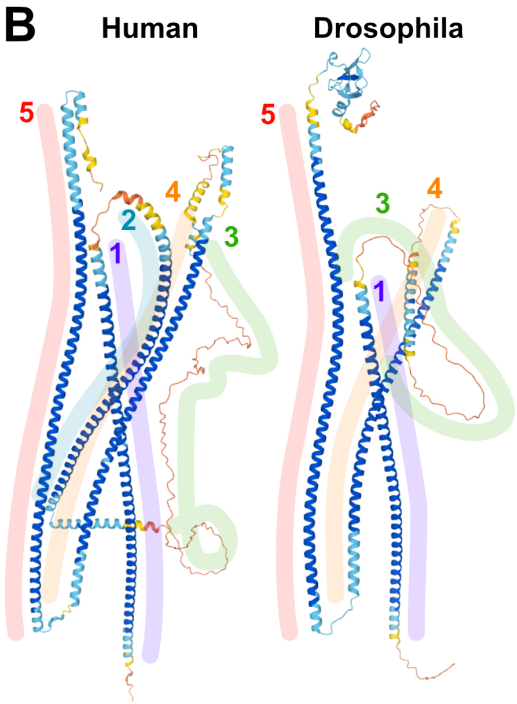

C

Alignment by predicted structural domain

		Identity	Similarity	Gaps
1	6 PASQPDVSLQQRVAELEKINAEFLRAQQQLEQEFNQKRAKFKELYLAKEEDLKRQNAVLQAAQDDLGHLRTQLWEAQAEM 85 17 PNGEDDATSQHKLSHLQ-------NEMRKMQNEFNTQRAKMRELYIQKEAE------VSQSQQE-----RRQL---QAEL 75 86 ENIKAIATVSENTKQEAIDEVKRQWREEVASLQAVMKETVRDYEHQFHLRLEQERTQWAQYRESAEREIA 155 H. s 76 DELKTHLMVADLKSQNELQLRDLKAQEEISSLQQLVQDTIEETAH-YKGEVERLRLELGKYQQIQQQTMA 144 D. m	25,33%	53,33%	14,67%
3	413 TSGSLQSKALGYNYKAKSAGNLDESDFGPLVGADSVSENF----DT--ASLG---------SLQMPSGFMLTKDQERAIK 477 151 SSGGIAPQVL--NQVKKTLGSVRK------LGTDSLNSSFQQDEDTRASSKGNGKQYAPEEAEMMHSIVEQLQEEMKALK 222 478 AMTPEQEE 485 H. s 223 VKLREQDE 230 D. m	23,86%	45,45%	26,14%
4	536 CSNYEKQLQGIQIQEAETRDQVKKLQLMLRQANDQLEKTMKDKQELEDFIKQSSEDSSHQISALVLRAQASEILLEELQQ 615 259 CSLAEKKTEELGAHINKQQKQVDLLQKQLVESRETLVKEAALRKDLEDQWQEKREAHKSEVQSLRDQAKTNEQRLLDMQQ 338 616 GLSQAKRDVQEQMAVLMQSREQVSEELVRLQKDNDSLQGKH 656 H. s 339 KFLETKDEVIKQIQRVSDDRERVNKQLETLQADNDFLSGRY 379 D. m	28,93%	55,37%	0,0%
5	677 LRELVLKYREDIINVRTAADHVEEKLKA---EILFLKEQIQAEQCLKENLEETLQLEIENCKEEIASISSLKAELERIKV 753 400 LQELILRQQSELIQARVSSEYERQKCTSTEDEIQILRAQLEESNNERRAYKRKMQLDIKSLQDR---VTEHLVTVQAYET 476 754 EKGQLESTLREKSQQLESLQEIKISLEEQLKKETAAKATVEQLMFEEKNKAQRLQTELDVSEQVQRDFVKLSQTLQVQLE 833 477 TKTQLERKEAELNKQLSECRVEIIELQEANEKYAKTNA-------DYKTKIKTLQEELSTMETVQKDFVKLSQTLQMSLE 549 834 RIRQADSLERIRAILNDTKLTDINQLP 860 H. s 550 ELRHADT--EVRWQDDD----DVNNCP 570 D. m	29,41%	51,87%	10,16%

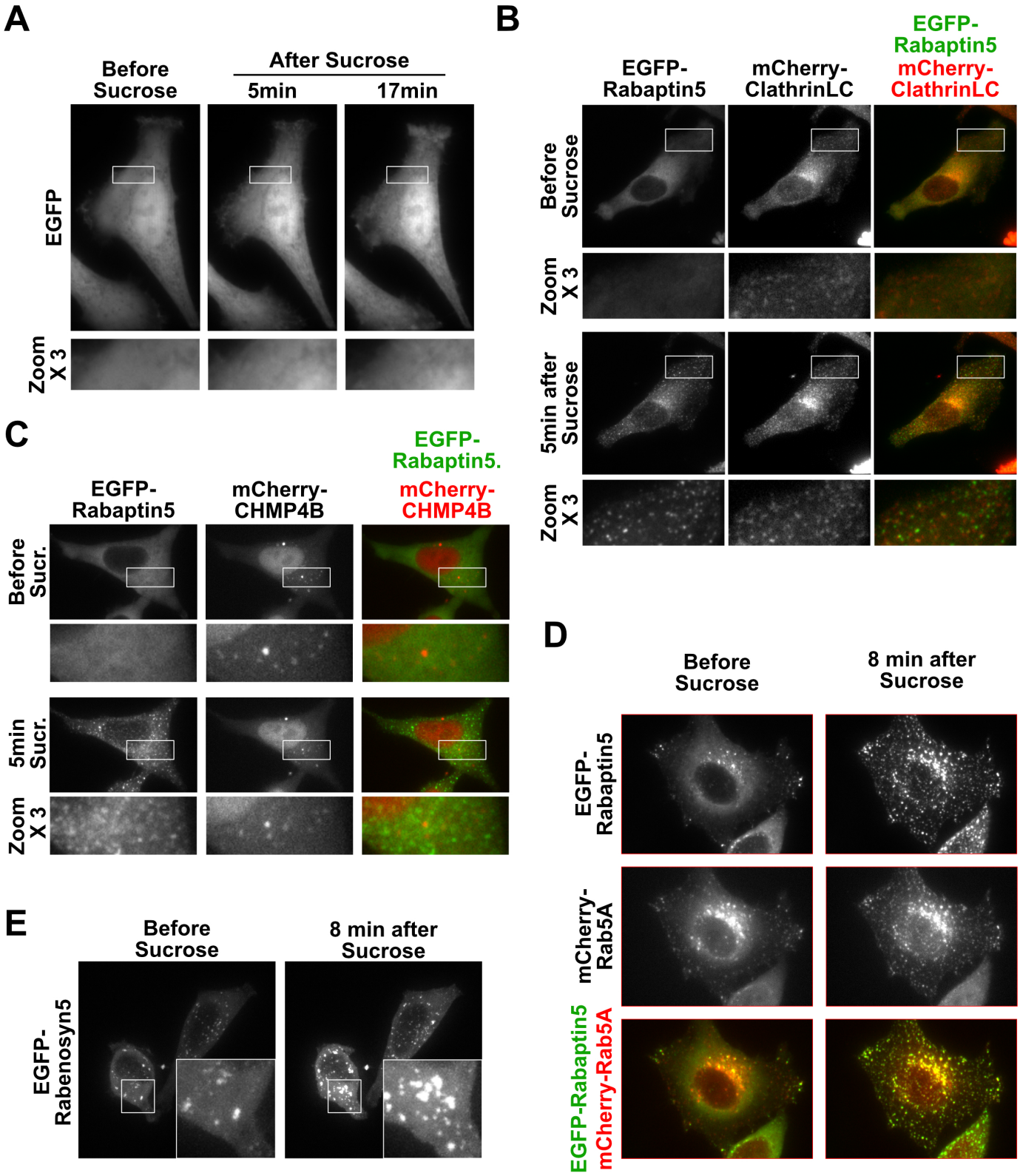
A
Before Sucrose
After Sucrose
5min
17min
EGFP
Zoom X 3
B
EGFP-Rabaptin5
mCherry-ClathrinLC
EGFP-Rabaptin5
mCherry-ClathrinLC
Before Sucrose
Zoom X 3
5min after Sucrose
Zoom X 3
C
EGFP-Rabaptin5
mCherry-CHMP4B
EGFP-Rabaptin5.
mCherry-CHMP4B
Before Sucr.
5min Sucr.
Zoom X 3
D
Before Sucrose
8 min after Sucrose
EGFP-Rabaptin5
mCherry-Rab5A
EGFP-Rabaptin5
mCherry-Rab5A
E
Before Sucrose
8 min after Sucrose
EGFP-Rabenosyn5

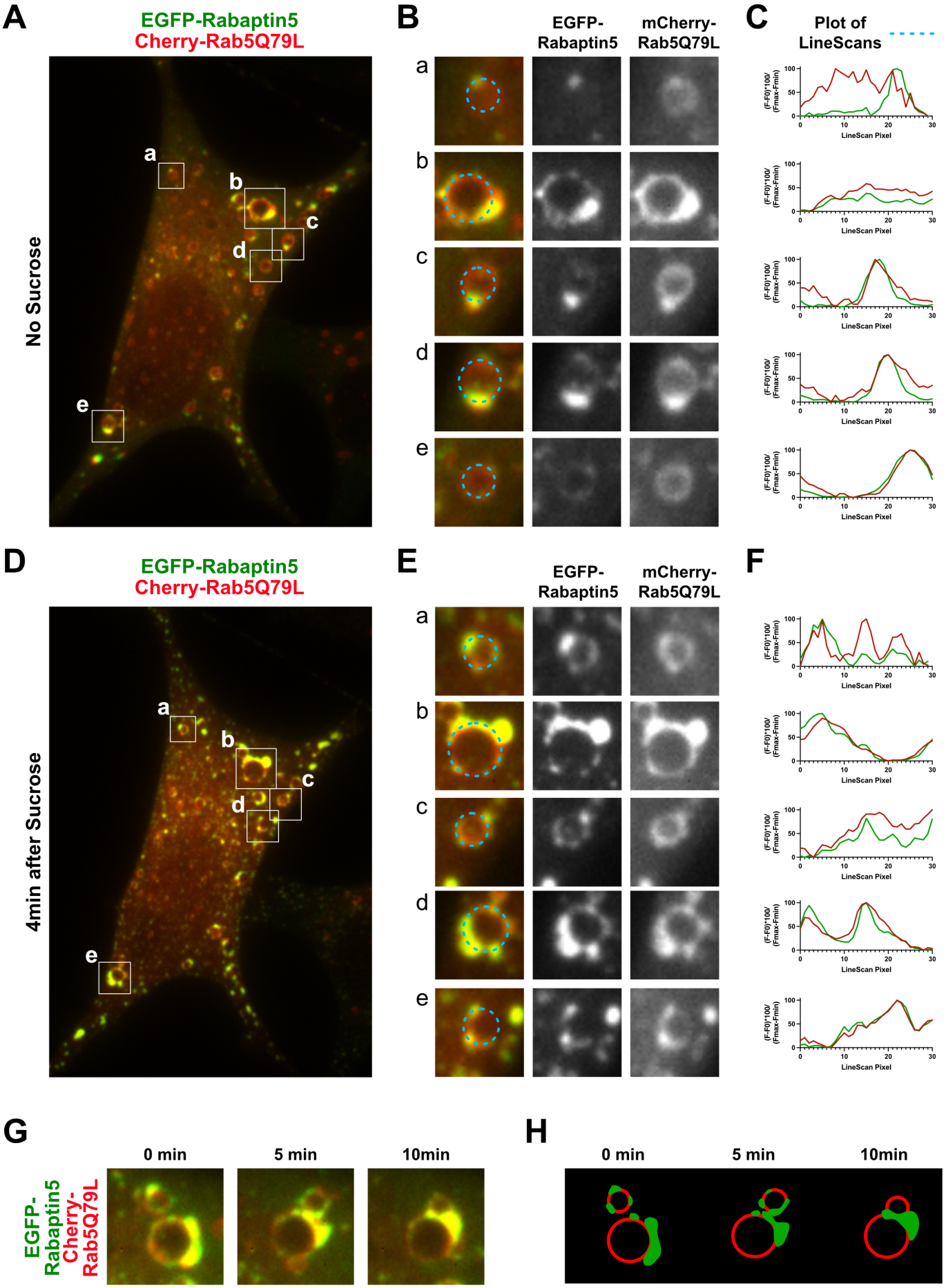
A
EGFP-Rabaptin5
Cherry-Rab5Q79L
No Sucrose
a
b
c
d
e
B
EGFP-Rabaptin5
mCherry-Rab5Q79L
C
Plot of LineScans
(F-F0)*100/(Fmax-Fmin)
LineScan Pixel
D
EGFP-Rabaptin5
Cherry-Rab5Q79L
4min after Sucrose
E
EGFP-Rabaptin5
mCherry-Rab5Q79L
F
G
0 min
5 min
10min
EGFP-Rabaptin5
Cherry-Rab5Q79L
H
0 min
5 min
10min

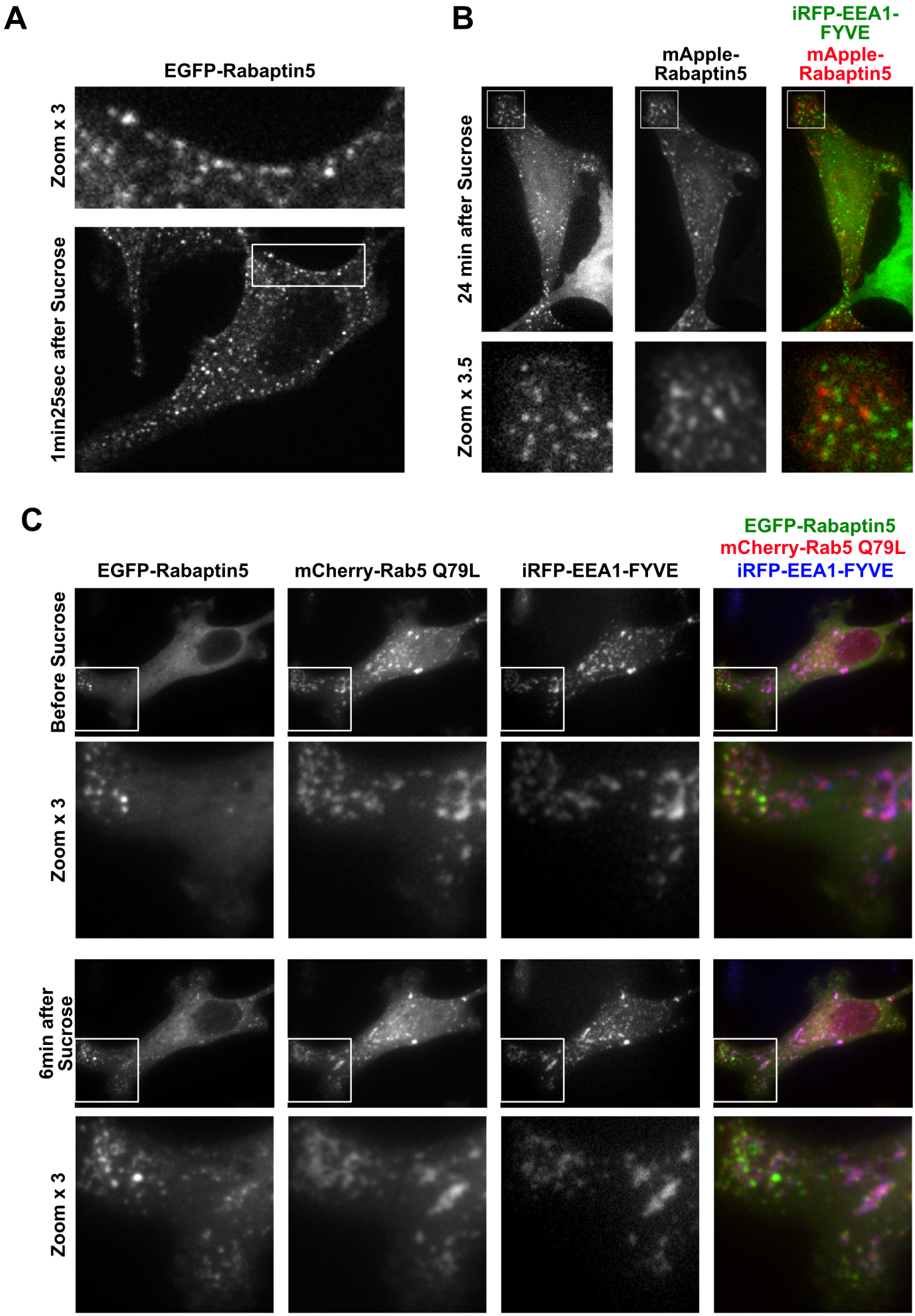
A
EGFP-Rabaptin5
Zoom x 3
1min25sec after Sucrose
B
mApple-Rabaptin5
iRFP-EEA1-FYVE
mApple-Rabaptin5
24 min after Sucrose
Zoom x 3.5
C
EGFP-Rabaptin5
mCherry-Rab5 Q79L
iRFP-EEA1-FYVE
EGFP-Rabaptin5
mCherry-Rab5 Q79L
iRFP-EEA1-FYVE
Before Sucrose
Zoom x 3
6min after Sucrose
Zoom x 3

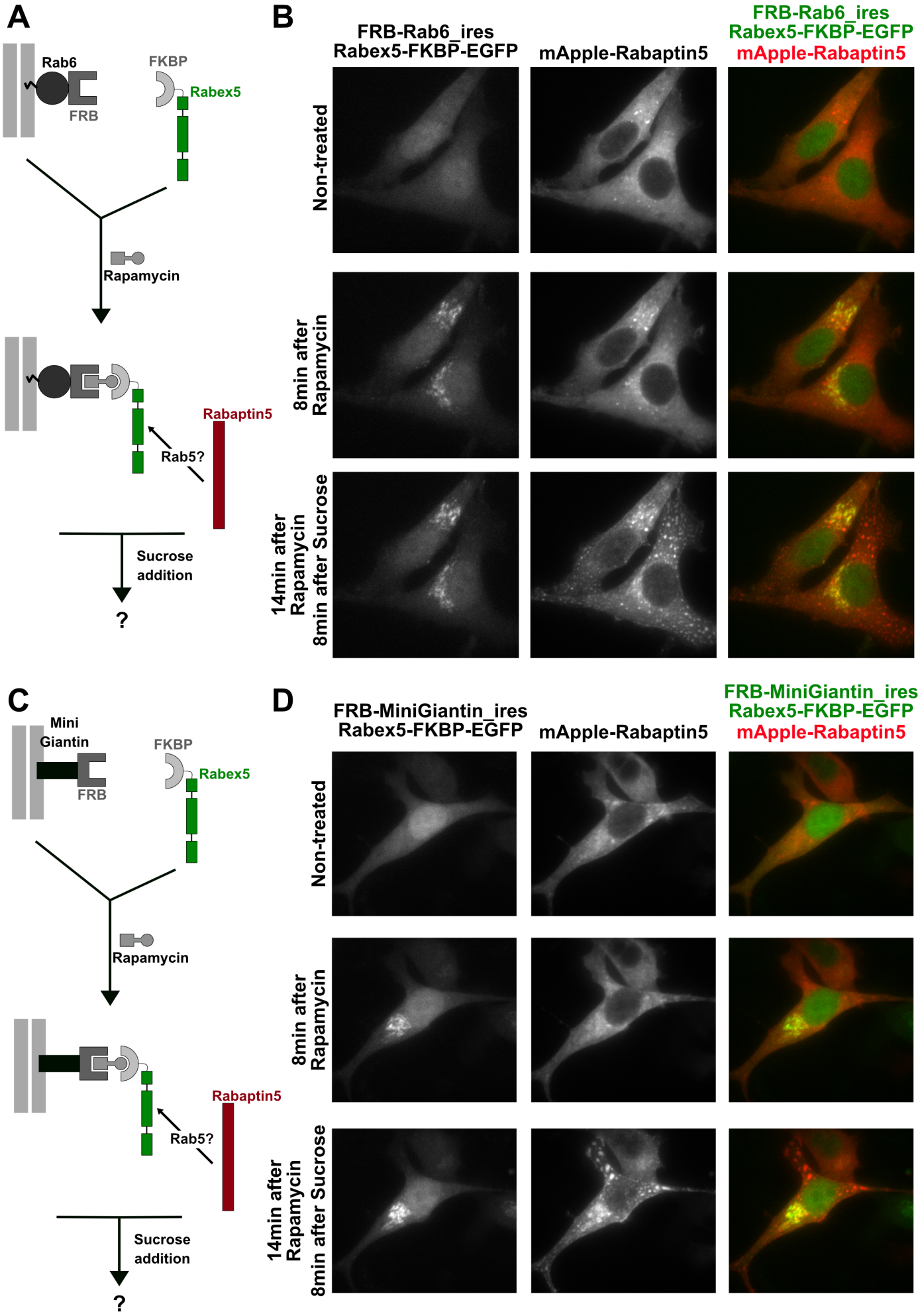
A
Rab6
FRB
FKBP
Rabex5
Rapamycin
Rabaptin5
Rab5?
Sucrose
addition
?
B
FRB-Rab6_ires
Rabex5-FKBP-EGFP
mApple-Rabaptin5
FRB-Rab6_ires
Rabex5-FKBP-EGFP
mApple-Rabaptin5
Non-treated
8min after
Rapamycin
14min after
Rapamycin
8min after Sucrose
C
Mini
Giantin
FRB
FKBP
Rabex5
Rapamycin
Rabaptin5
Rab5?
Sucrose
addition
?
D
FRB-MiniGiantin_ires
Rabex5-FKBP-EGFP
mApple-Rabaptin5
FRB-MiniGiantin_ires
Rabex5-FKBP-EGFP
mApple-Rabaptin5
Non-treated
8min after
Rapamycin
14min after
Rapamycin
8min after Sucrose

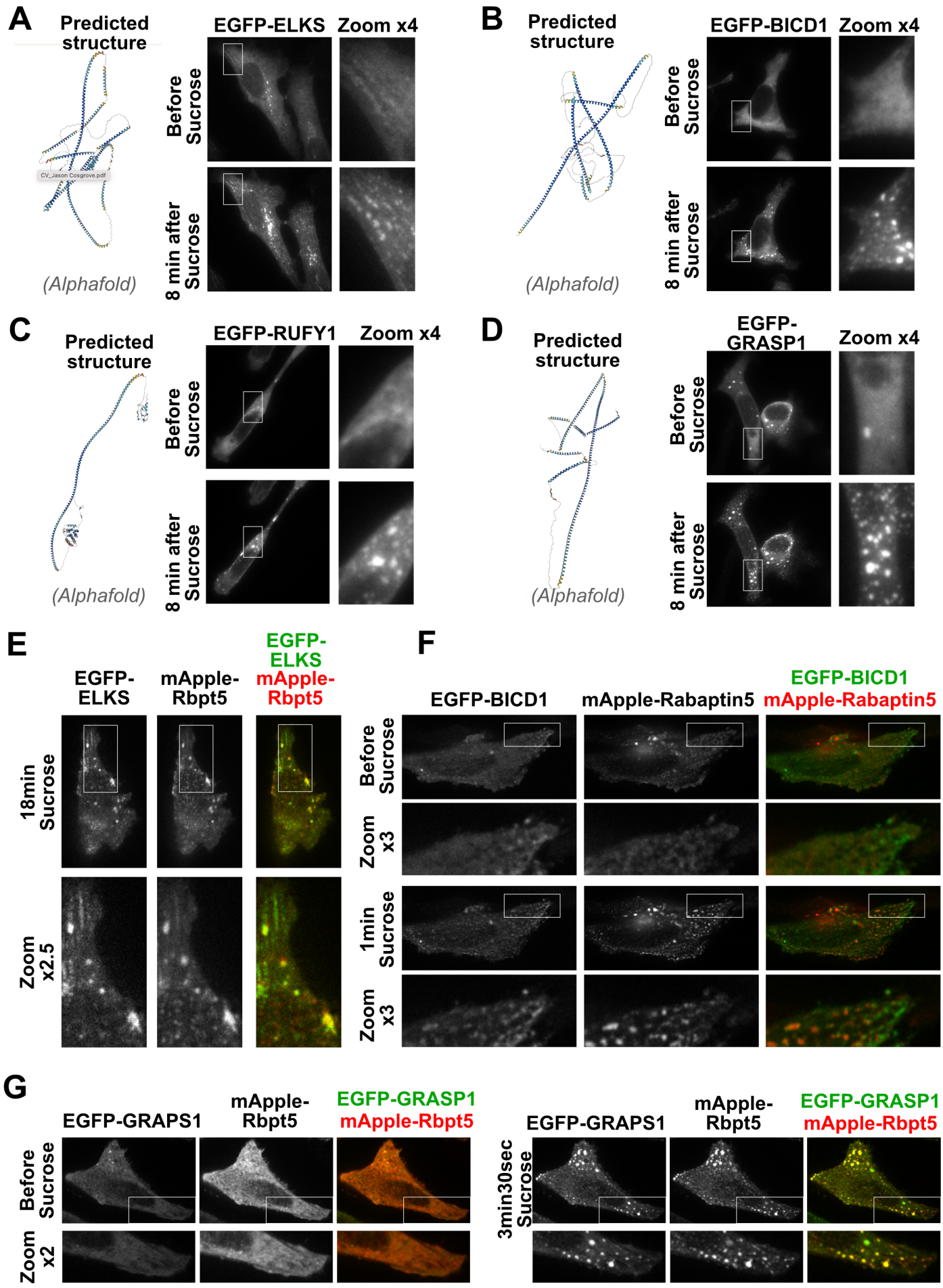
A
Predicted structure
(Alphafold)
EGFP-ELKS
Zoom x4
Before Sucrose
8 min after Sucrose
B
Predicted structure
(Alphafold)
EGFP-BICD1
Zoom x4
Before Sucrose
8 min after Sucrose
C
Predicted structure
(Alphafold)
EGFP-RUFY1
Zoom x4
Before Sucrose
8 min after Sucrose
D
Predicted structure
(Alphafold)
EGFP-GRASP1
Zoom x4
Before Sucrose
8 min after Sucrose
E
EGFP-ELKS
mApple-Rbpt5
EGFP-ELKS mApple-Rbpt5
18min Sucrose
Zoom x2.5
F
EGFP-BICD1
mApple-Rabaptin5
EGFP-BICD1 mApple-Rabaptin5
Before Sucrose
Zoom x3
1min Sucrose
Zoom x3
G
EGFP-GRAPS1
mApple-Rbpt5
EGFP-GRASP1 mApple-Rbpt5
Before Sucrose
Zoom x2
EGFP-GRAPS1
mApple-Rbpt5
EGFP-GRASP1 mApple-Rbpt5
3min30sec Sucrose

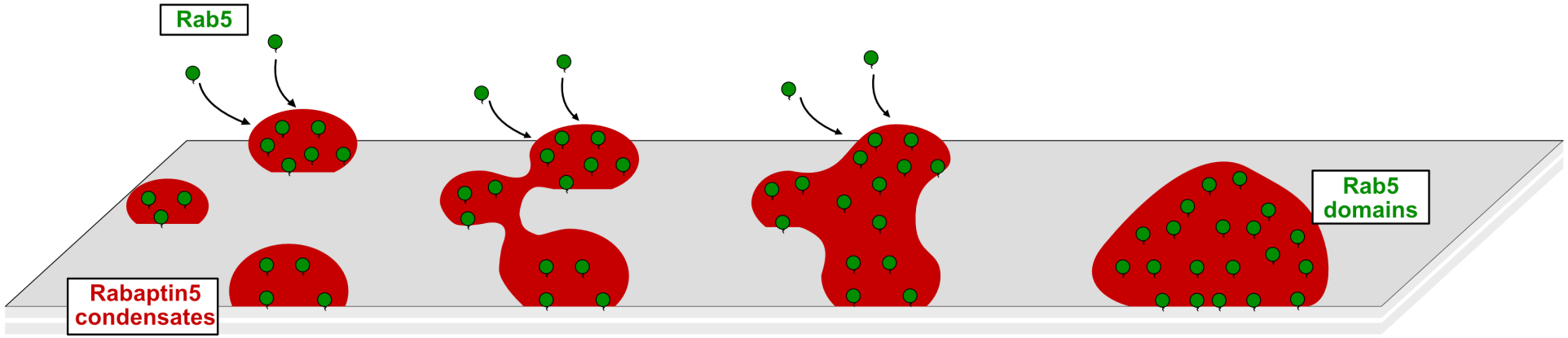
Rab5
Rab5 domains
Rabaptin5 condensates

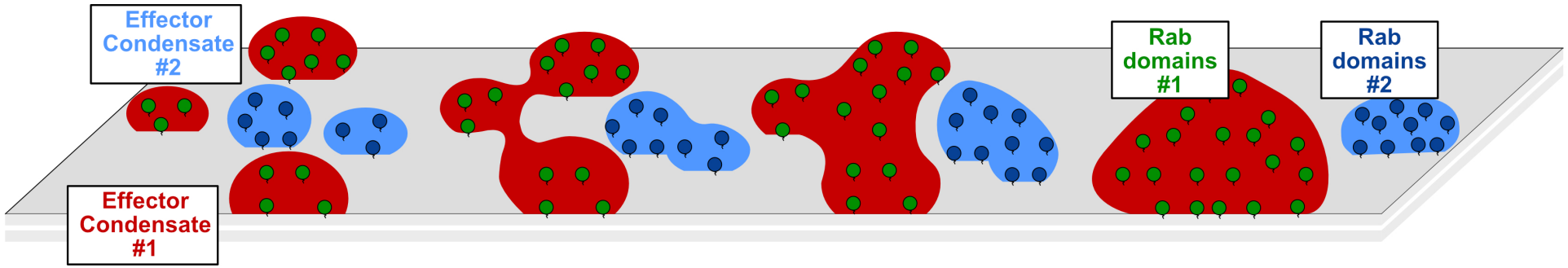
Effector Condensate #2
Rab domains #1
Rab domains #2
Effector Condensate #1